SUPPLEMENTARY INFORMATION

Rationalising Catalytic Performance using a Unique Correlation Matrix

Maciej G. Walerowski[a], Stylianos Kyrimis[a,b], Victoria Hewitt[a], Lindsay-Marie Armstrong[b] and Robert Raja[a*]

[a] School of Chemistry, University of Southampton, Southampton, SO17 1BJ, UK.

[b] School of Engineering, University of Southampton, Southampton, SO17 1BJ, UK.

*R.Raja@soton.ac.uk

1 Synthetic protocols

1.1 SAPO-34

A large batch of SAPO-34 was synthesised as follows, as per published approaches.[1] TEAOH (91.06 g, 35 wt% in H_2O, Sigma-Aldrich) was added to a 1 L Teflon beaker. Aluminium isopropoxide (45.16 g, ≥98%, Sigma-Aldrich) was then slowly added to the TEAOH solution and mixed for 1 hour. Silica fumed (1.99 g, Sigma-Aldrich) was then slowly added to the beaker and mixed for a further 1 hour. Deionised water (35.94 g, 0.8 µS/cm, VWR Water GPR Rectapur) and phosphoric acid (25.27, ≥85wt% in H_2O, Sigma-Aldrich) were gently mixed in a separate glass beaker and then added dropwise into the Teflon beaker and mixed for a further 2 hours. The uniform white gel of ratio 1.0Al:1.0P:0.15Si:1.0TEAOH:9H_2O was then crystallised in a Teflon lined Parr batch reactor at 200°C for 72 hours with no mixing. Once crystallisation was complete, the Parr reactor was immediately quenched in ice. White solid was then separated via centrifugation and washed twice with DI water. The white solid was then dried overnight in a 70°C oven to yield a fine, white crystalline material. The material was then calcined at 600°C for 16 hours in flowing air with a 2.5°C/min ramp rate to yield a white crystalline material.

1.2 Cu^0-ZnO/SAPO-34

Cu^0-ZnO/SAPO-34 bifunctional catalysts with a Cu:Zn:SAPO-34 mass ratio of either 2:1:10, 1:0.5:10 or 0.5:0.25:10 were made as follows. Deionised water (15, 30 or 45 mL, 18.2 MΩ), ethanol (45 mL, 99.8%, Fisher) or acetone (45 mL, ACS reagent, Sigma-Aldrich), copper (II) acetate monohydrate (98+% extra pure, Acros Organics) & zinc acetate dihydrate (98% extra pure, Acros Organics) were added to a RBF situated in a 70°C oil bath and mixed for 15 minutes. Calcined SAPO-34 was then added to the dark blue clear solution and mixed for further 30 minutes. The mixture was then evaporated to dryness at 50, 80 or 120°C, and the resulting pale green powder was then calcined at 300°C for 5 hours in flowing air with a 2.5°C/min ramp rate to yield a fine brown material and reduced at 300°C for 4 hours in 300 mL/min H_2 in N_2 flow with a 2.5°C/min ramp rate to yield a dark brown/pale black material. The samples were stored in a desiccator under a nitrogen atmosphere.

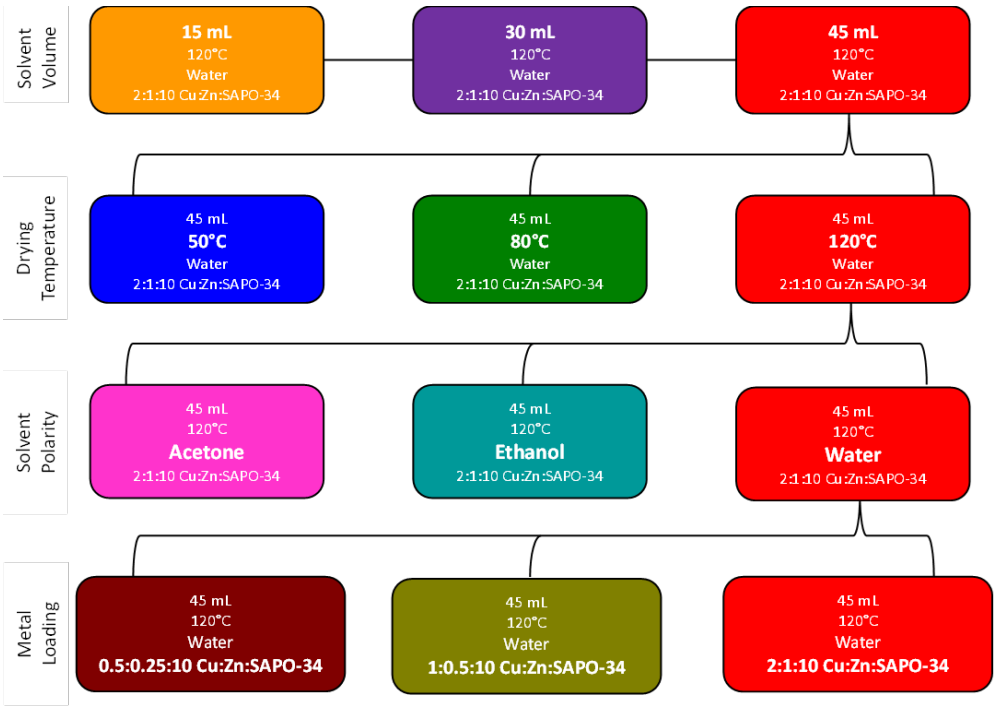

Fig. S1 Schematic outlining the procedure used to synthesise different Cu^0-ZnO/SAPO-34 catalyst by changing one variable at a time.

2 Characterisation protocols

2.1 Elemental analysis

Inductively coupled plasma – mass spectrometric (ICP-MS) analysis was performed at the School of Ocean and Earth Science, University of Southampton. Samples (~10 mg) were fully digested in a hot mixture of concentrated HCl (1 mL), HNO_3 (1 mL) and HF (0.75 mL) overnight. Digested solutions were subsequently diluted in water and then sub sampled and further diluted with 3% HNO_3 to give an approximate dilution of 1 million, and spiked to give Be at 20ppb, and Ru and Re at 5 ppb to act as internal standards. The samples were analysed on a ThermoFisher XSeries2 ICP-MS operating in standard and CCT modes. Calibration was carried out using synthetic standards prepared from Inorganic Venture single element ICP-MS standards and the standards were also spiked to give the same concentration of internal standards as for the samples.

2.2 Powder X-ray diffraction (XRD)

PXRD characterisation was performed using a Bruker D2 Phaser instrument. Patterns were obtained using Cu Kα radiation (λ = 1.54184 Å) at 30 kV voltage and 10 mA current using a 0.6 mm slit. Patterns were obtained in the 5-60° 2θ range with 0.02° increments and 0.2 s per step.

2.3 Surface area and porosity

Surface area and porosity characterisation was performed using Micromeritics Tristar II 3020 analyser. N_2 was used as the adsorptive, and a liquid N_2 bath was utilised. Analysis performed between 0.00 and 0.95 p/p_0 (relative pressure). 124 adsorption and 30 desorption points were used to obtain the full physisorption isotherm. BET surface area and pore volume calculated automatically by the Micromeritics Tristar II 3020 software. Samples (~0.15 g) were thoroughly degassed for a minimum of 21 hours using a Micrometrics Vac Prep 062 system by heating them under vacuum at 120°C, with final pressure of ~100 mTorr.

2.4 Transmission electron microscopy (TEM)

TEM imaging was performed using a Hitachi HT7700 instrument at an acceleration voltage of 100 kV. The instrument was equipped with a Morada G3 (16 MP) detector for digital imaging. The sample powder was suspended in ethanol and loaded directly onto carbon and formvar coated copper TEM grids. The characterisation was performed at the Biological Imaging Unit at the University Hospital Southampton.

2.5 X-ray absorption spectroscopy (XAS)

The XAS spectra for the Cu and Zn K-edges (8.979 and 9.659 keV respectively) were collected at the general purpose XAS beamline, B18 at the Diamond Light Source (UK) and accessed through the UK Catalysis Hub, block allocation group (BAG, SP34632-1 and SP34632-2). The collimated, white X-ray beam is incident on a Si(111) double crystal monochromator and a Pt-coated focusing mirrors, covering the energy range 6.34 keV to 9.98 keV. The beam size at the sample was approximately 1.0 x 1.0 mm^2 (V x H) and the photon flux was ~1011 ph/s (no attenuation). The XAS spectra were collected in transmission mode and the intensity of the incident beam (I_0) and the transmitted beam (I_t) was monitored by ionization chambers (filled with a mixture of He, N_2, and Ar). Samples (~30 mg) were diluted with cellulose (~30 mg) before pressing into 13mm diameter pellets. The XAS spectra of each sample were measured at least 2 times in transmission mode at room temperature and merged to improve the signal-to-noise ratio. Zn and Cu metal foil was measured simultaneously for each sample as a reference for energy calibration. XAS data was analysed using the Demeter software package which includes Athena and Artemis.[2]

3 Catalysis protocols

Catalysis was performed in a custom built reactor which comprised of hydrogen, argon and carbon dioxide cylinders, three mass flow controllers, laptop computer to control the mass flow controllers and mass spectrometer, heating jacket for the reactor, emergency proportional pressure relief valve, pressure gauge, backpressure regulator, hotplate to heat the backpressure regulator and a mass spectrometer. Temperature, gas flow rate and mass spectrometric calibrations were performed previously to ensure accurate results and quantification.

Catalyst powder (~0.4 g) was pelletised at 4 tonnes using a Graseby Specac pellet press for 10 seconds to yield self-supporting discs of 2.5 cm diameter. The discs were then crushed and sieved 5 times between 300 and 500 µm sieves to yield catalyst particles in the 300-500 µm range. The catalyst particles (0.300 g) were then sandwiched between 5 and 17 cm layers of 1 mm borosilicate beads and the reactor placed inside the heating jacket.

The catalyst was then reduced in a 60 mL/min H_2 flow at 300°C for 2 hours before temperature was reduced to 260°C. Reaction gas mixture of 5.5 Ar, 15 CO_2 and 45 H_2 mL/min was flown into the reactor and pressure was built up to 40 bars. As soon as the reaction pressure was attained, mass spectrometric analysis was started. The reaction was allowed to proceed for a minimum of 3 hours after which steady state was obtained. Mass spectrometric measurements were taken every ~10 seconds and the results presented are an average over a period of 15 minutes which is approximately equal to 100 analysis points. Argon was used as an internal standard. Each experiment was performed in triplicate, using fresh catalyst on a different day in a randomised order. Standard deviation was calculated between the three repeats to give error in each result.

Equations S1-S3 were used to calculate product selectivity. Equation S4 was used to calculated carbon mass balance by comparing the inlet and outlet moles of carbon. Equation S5 was used to calculate the metal time yield.

$$\textbf{Equation S1}\ CO\ Selectivity = \frac{n_{CO}}{\sum n_{(CO+MeOH+2DME)}}\ x\ 100$$

$$\textbf{Equation S2}\ MeOH\ Selectivity = \frac{n_{MeOH}}{\sum n_{(CO+MeOH+2DME)}}\ x\ 100$$

$$\textbf{Equation S3}\ DME\ Selectivity = \frac{2n_{DME}}{\sum n_{(CO+MeOH+2DME)}}\ x\ 100$$

$$\textbf{Equation S4}\ Carbon\ Mass\ Balance = \frac{\sum n_{(CO_2\ out+CO+MeOH+2DME)}}{nCO_{2\ in}}$$

$$\textbf{Equation S5}\ Metal\ Time\ Yield = \frac{n_{Product}\ x\ M_{Product}}{m_{Metal}}\ x\ 60$$

Where the $CO_{2\ in}$ and $CO_{2\ out}$ are the inlet and outlet molar flow rates (mol/min) of CO_2 respectively, n (mol/min) is the outlet molar flow rate of the species of interest, M is the molar mass of the species of interest (mol g^{-1}) and m_{Metal} is the total mass of zinc and copper (kg) in the catalyst used for catalysis.

4 Results

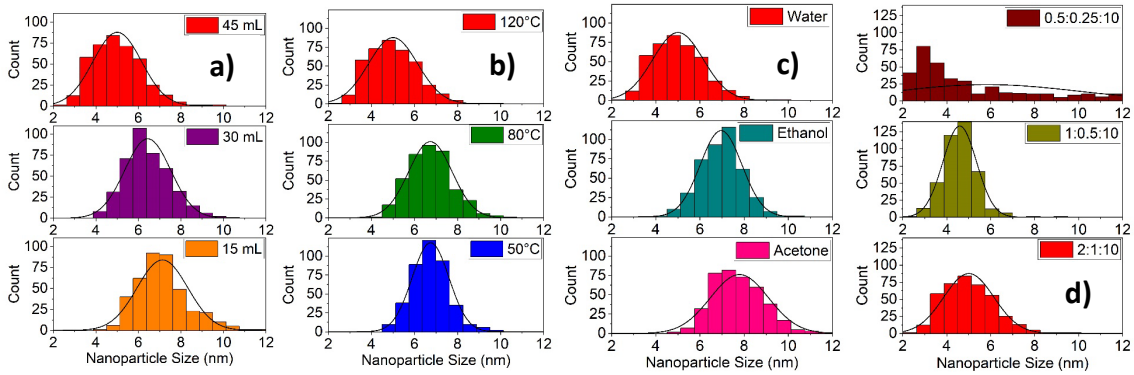

Fig. S2 Impact of **a)** solvent volume **b)** drying temperature **c)** solvent polarity and **d)** metal loading on TEM-derived nanoparticle sizes of the Cu^0-ZnO/SAPO-34 catalyst. Results based on a measurement of >400 nanoparticles.

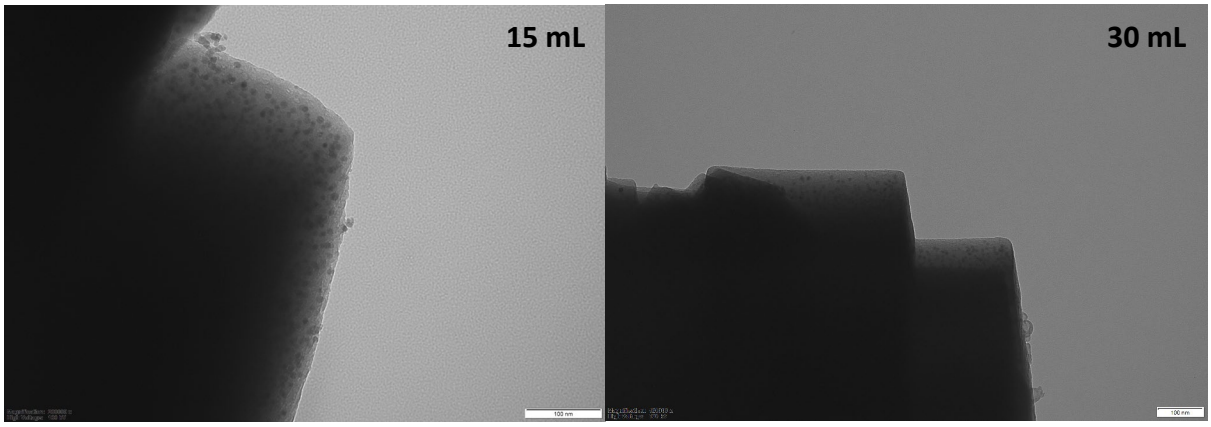

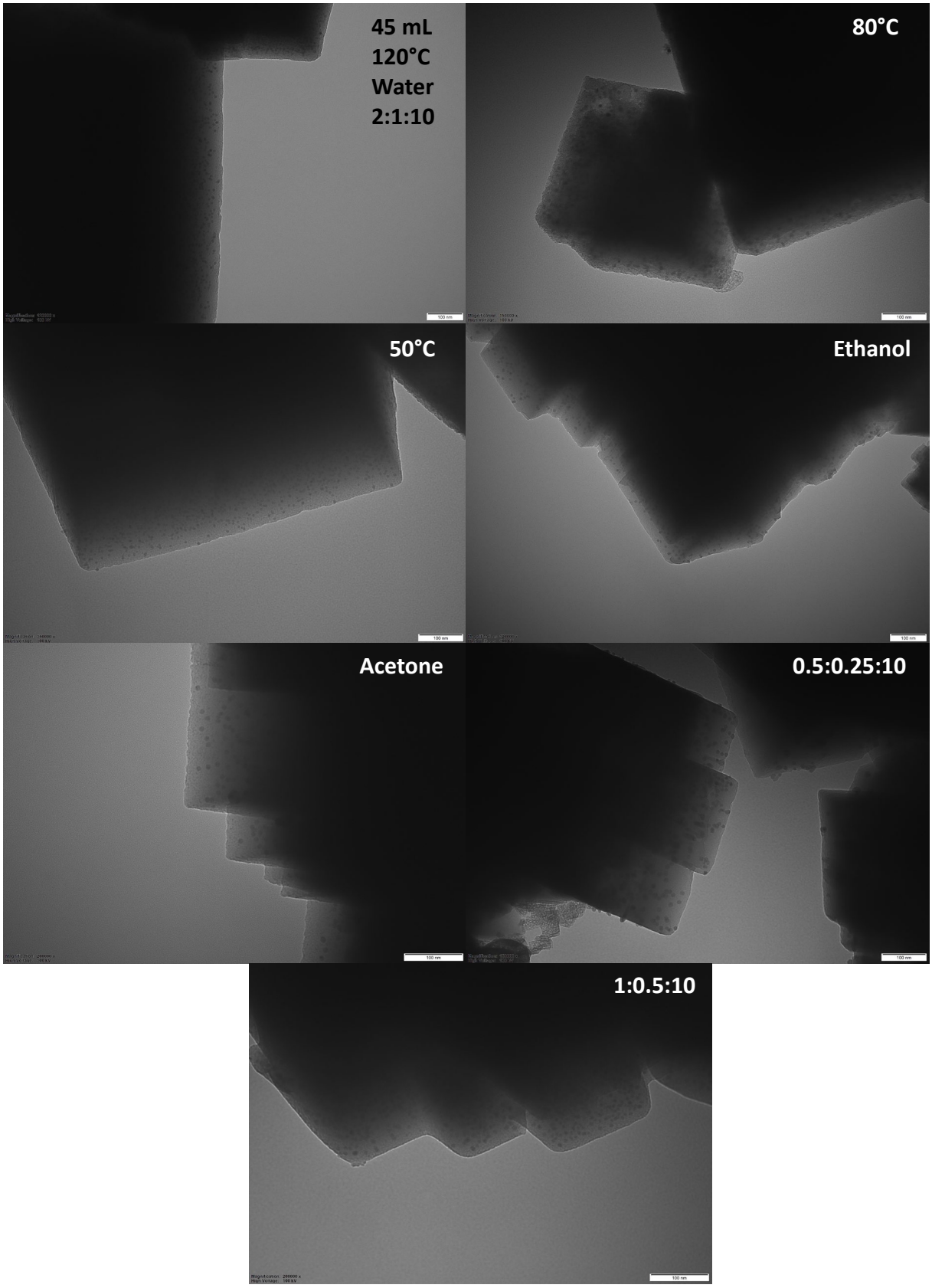

Fig. S3 TEM images of Cu^0-ZnO/SAPO-34 catalysts showing the impact of synthesis modification on the Cu^0-ZnO nanoparticle size.

Table S1 EXAFS Fitting for Cu K-edge data of Cu^0-ZnO/SAPO-34 catalysts prepared via various synthetic methods.

Synthesis Method	Scattering Path	Coordination number	$2\sigma^2$ (Å^2)	*R* (Å)	E_f (eV)	*R* factor
15 mL	Cu-Cu	9.2 (2)	0.0180 (4)	2.541 (3)	4.3 (5)	0.002
	Cu-O	0.5 (1)	0.008 (6)	1.88 (2)		
30 mL	Cu-Cu	8.5 (2)	0.0186 (4)	2.539 (3)	4.1 (5)	0.002
	Cu-O	0.6 (1)	0.010 (6)	1.88 (2)		
45 mL / 120°C	Cu-Cu	7.4 (2)	0.0186 (6)	2.539 (5)	4.0 (8)	0.003
	Cu-O	1.0 (1)	0.012 (4)	1.88 (1)		
50°C	Cu-Cu	8.7 (1)	0.0180 (2)	2.539 (3)	4.2 (4)	0.001
	Cu-O	0.47 (8)	0.008 (6)	1.88 (2)		
80°C	Cu-Cu	8.4 (2)	0.0180 (4)	2.541 (4)	4.3 (6)	0.002
	Cu-O	0.6 (1)	0.008 (6)	1.88 (2)		
Water / 2:1:10	Cu-Cu	6.9 (2)	0.0184 (6)	2.539 (5)	4.3 (9)	0.004
	Cu-O	1.2 (1)	0.012 (4)	1.88 (1)		
Ethanol	Cu-Cu	7.4 (2)	0.0180 (6)	2.540 (5)	4.2 (8)	0.003
	Cu-O	1.1 (1)	0.012 (4)	1.88 (1)		
Acetone	Cu-Cu	9.1 (2)	0.0182 (2)	2.538 (3)	4.2 (4)	0.001
	Cu-O	0.45 (8)	0.008 (6)	1.88 (2)		
0.5:0.25:10	Cu-Cu	5.0 (4)	0.019 (1)	2.54 (1)	5 (2)	0.012
	Cu-O	2.2 (2)	0.014 (2)	1.90 (2)		
1:0.5:10	Cu-Cu	7.0 (2)	0.0190 (6)	2.537 (5)	4.2 (9)	0.003
	Cu-O	1.3 (1)	0.012 (4)	1.88 (1)		

Amplitude reduction factor of 0.86 was determined from fitting of Cu^0 with fixed CN of 12. Values in brackets indicate error (±) in the last reported significant figure.

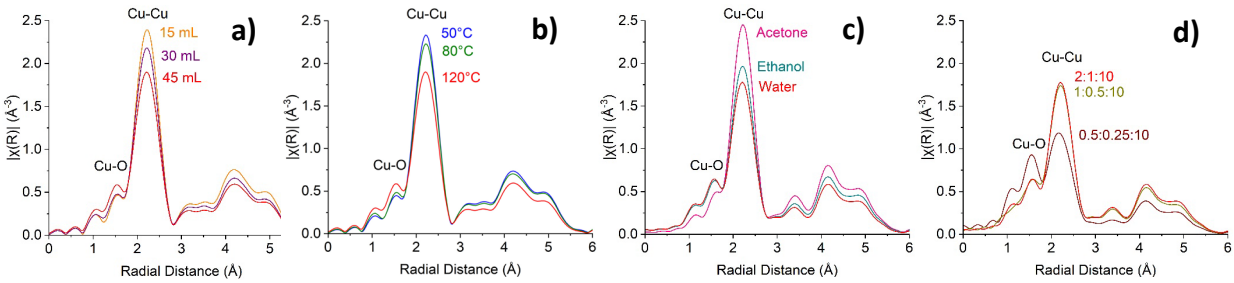

Fig. S4 Impact of **a)** solvent volume **b)** drying temperature **c)** solvent polarity and **d)** metal loading on the Fourier transformed k2-weighted X Cu K Edge EXAFS data.

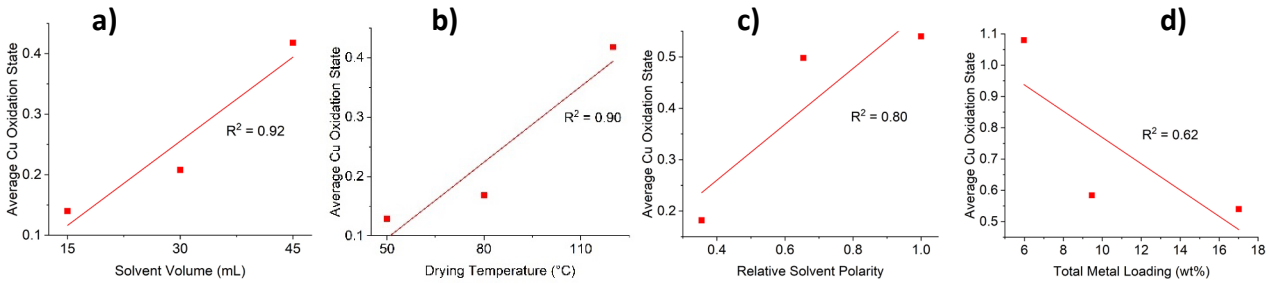

Fig. S5 Impact of **a)** solvent volume **b)** drying temperature **c)** solvent polarity and **d)** metal loading on average Cu oxidation state of the Cu^0-ZnO/SAPO-34 catalyst. Fitting data for the oxidation state can be found in Table S3.

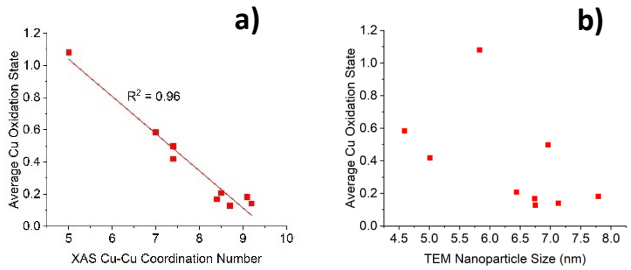

Fig. S6 Correlation between XAS-derived Cu oxidation state and **a)** XAS-derived Cu-Cu coordination number and **b)** TEM-derived nanoparticle size.

Table S2 EXAFS Fitting for Zn K-edge data of Cu^0-ZnO/SAPO-34 catalysts prepared via various synthetic methods.

Synthesis Method	Scattering Path	Coordination number	$2\sigma^2$ (Å^2)	*R* (Å)	E_f (eV)	*R* factor
15 mL	Zn-O	5.7 (2)	0.018 (1)	1.965 (9)	1.3 (9)	0.034
	Zn-Zn	12 (3)	0.056 (6)	3.28 (2)		
30 mL	Zn-O	5.13 (4)	0.0140 (2)	1.964 (2)	1.6 (2)	0.002
	Zn-Zn	9.0 (4)	0.039 (1)	3.254 (3)		
45 mL / 120°C	Zn-O	5.02 (7)	0.0134 (4)	1.963 (3)	1.9 (3)	0.004
	Zn-Zn	9.4 (6)	0.039 (1)	3.256 (5)		
50°C	Zn-O	5.4 (1)	0.0158 (6)	1.965 (4)	1.4 (5)	0.009
	Zn-Zn	8 (1)	0.048 (4)	3.29 (1)		
80°C	Zn-O	5.5 (3)	0.018 (2)	1.97 (1)	2 (2)	0.085
	Zn-Zn	8 (4)	0.052 (1)	3.32 (5)		
Water / 2:1:10	Zn-O	5.20 (6)	0.0140 (4)	1.961 (3)	1.8 (3)	0.004
	Zn-Zn	9.4 (5)	0.040 (1)	3.254 (5)		
Ethanol	Zn-O	5.4 (1)	0.0146 (6)	1.964 (4)	1.6 (5)	0.009
	Zn-Zn	10.1 (7)	0.035 (2)	3.240 (7)		
Acetone	Zn-O	5.2 (1)	0.0142 (6)	1.967 (5)	1.4 (5)	0.011
	Zn-Zn	10.0 (8)	0.036 (2)	3.243 (7)		
0.5:0.25:10	Zn-O	5.8 (1)	0.0174 (6)	1.970 (5)	0.8 (5)	0.007
	Zn-Zn	8.4 (7)	0.035 (2)	3.240 (7)		
1:0.5:10	Zn-O	5.38 (9)	0.0150 (6)	1.965 (4)	1.5 (4)	0.006
	Zn-Zn	9.2 (6)	0.035 (1)	3.245 (6)		

Amplitude reduction factor of 0.693 was determined from fitting of Zn^0 using two Zn-Zn paths with bond lengths of 2.665 and 2.913 Å each with a coordination number of 6.

Table S3 Average XAS-derived oxidation states of Cu^0-ZnO/SAPO-34 catalysts prepared via various synthetic methods.

Synthesis Method	Average Cu oxidation state	R Factor for Cu LCF	Average Zn oxidation state	R Factor for Zn LCF
15 mL	0.14	0.001	1.93	0.054
30 mL	0.21	0.001	1.99	0.046
45 mL / 120°C	0.42	0.001	1.92	0.044
50°C	0.13	0.020	1.95	0.059
80°C	0.17	0.002	1.93	0.062
Water/ 2:1:10	0.54	0.001	1.87	0.045
Ethanol	0.50	0.001	1.97	0.038
Acetone	0.18	0.001	1.95	0.409
0.5:0.25:10	1.1	0.003	2.00	0.050
1:0.5:10	0.58	0.002	1.93	0.046

Table S4 Copper and zinc loading of the Cu^0-ZnO/SAPO-34 catalysts prepared via different synthetic approaches.

Catalyst	Cu Loading (wt%)	Zn Loading (wt%)	Cu/Zn Mass Ratio
15 mL	11.3	5.4	2.1
30 mL	10.9	5.2	2.1
45 mL/120°C/ Water/2:1:10	11.6	5.4	2.1
50°C	13.3	5.5	2.4
80°C	11.6	5.6	2.1
Ethanol	12.1	6.0	2.0
Acetone	11.9	5.5	2.2
0.5:0.25:10	3.9	2.1	1.9
1:0.5:10	6.4	3.1	2.1

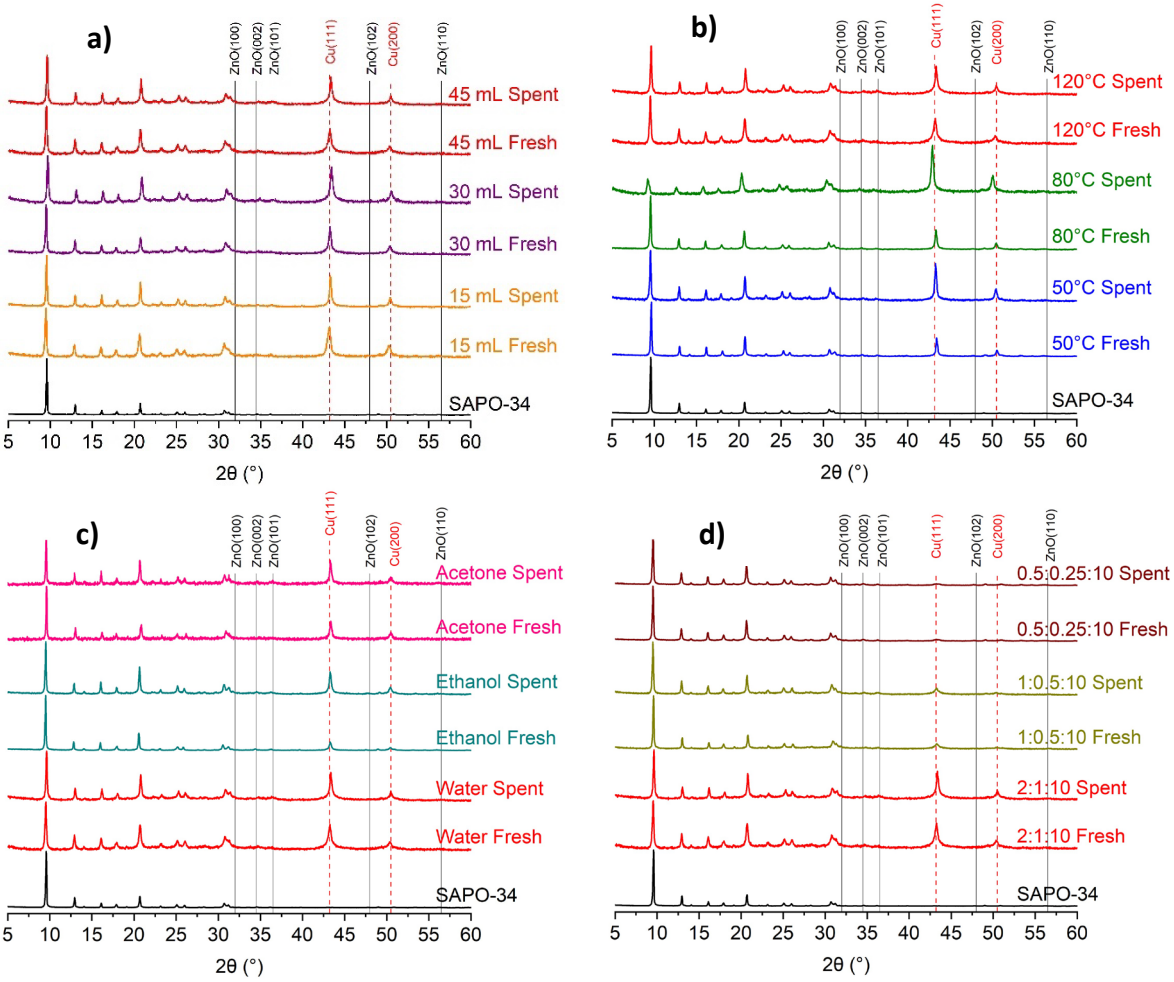

Fig. S7 XRD patterns of fresh and spent Cu^0-ZnO/SAPO-34 catalysts synthesised with different **a)** solvent volume **b)** drying temperature **c)** solvent polarity and **d)** metal loading.

Table S5 Surface area and pore volumes of the Cu^0-ZnO/SAPO-34 catalysts prepared via different synthetic approaches.

Catalyst	Total Surface Area (m^2/g)	Micropore Surface Area (m^2/g)	Total Pore Volume (cm^3/g)	Micropore Pore Volume (cm^3/g)
15 mL	323	292	0.19	0.15
30 mL	292	270	0.17	0.14
45 mL/120°C/ Water/2:1:10	302	275	0.18	0.14
50°C	320	284	0.19	0.14
80°C	308	271	0.18	0.13
Ethanol	335	311	0.20	0.16
Acetone	314	295	0.18	0.15
0.5:0.25:10	397	373	0.21	0.19
1:0.5:10	367	350	0.20	0.18

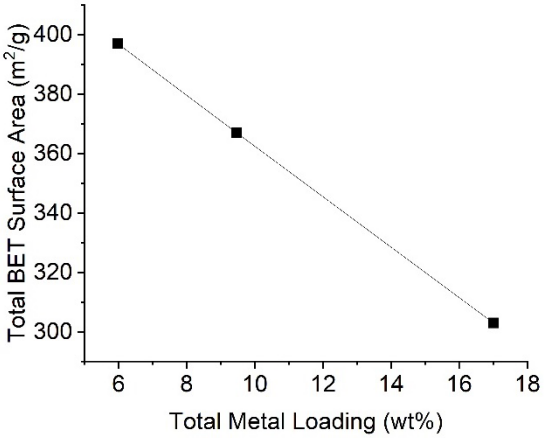

Fig. S8 Impact of metal loading on the total surface area of the Cu^0-ZnO/SAPO-34 catalyst.

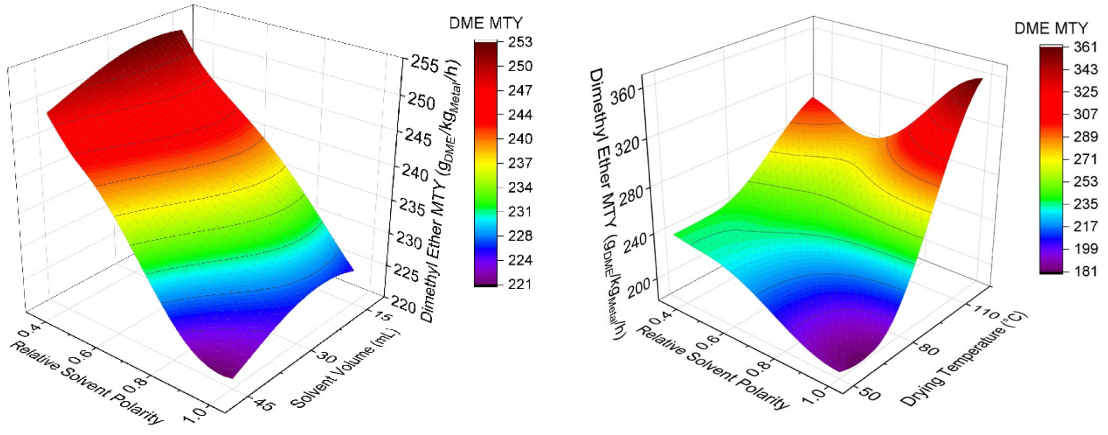

Fig. S9 Three dimensional model response surface models showing the impact of different synthesis conditions on predicted DME metal time yield.

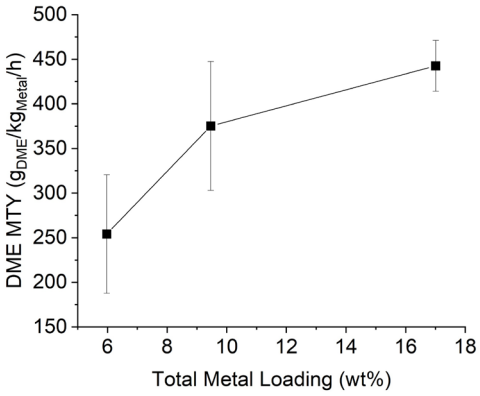

Fig. S10 Impact of metal loading on the experimentally observed DME metal time yield.

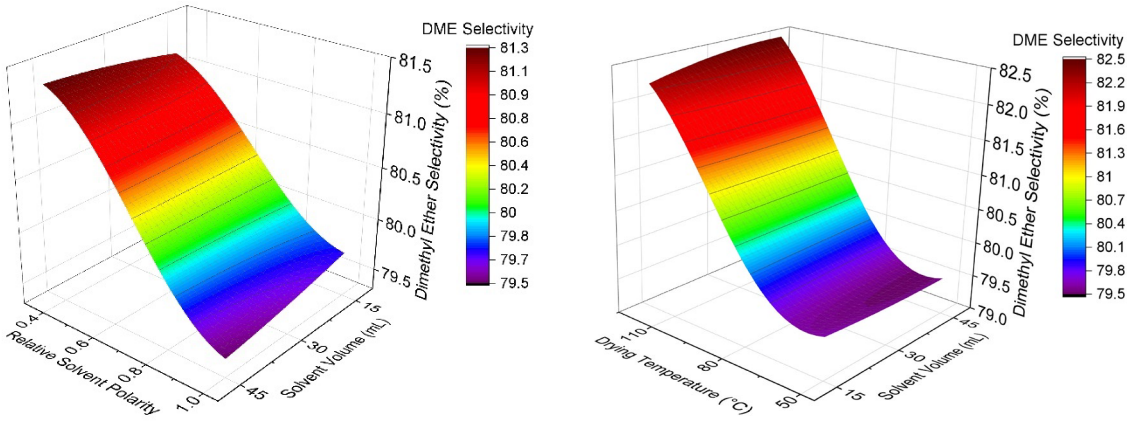

Fig. S11 Three dimensional response surface models showing the impact of different synthesis conditions on predicted DME selectivity.

Table S6 Surface area and pore volumes of the fresh pelletised and spent pelletised Cu^0-ZnO/SAPO-34 catalysts prepared via different synthetic approaches showing the decrease in surface area due to coking.

Catalyst	Fresh Pelletised Surface Area (m2/g)	Spent Pelletised Surface Area (m2/g)	Surface Area Lost (m2/g)	Surface Area Lost (%)
15 mL	277	258	19	6.9
30 mL	264	233	31	11.7
45 mL/120°C/ Water/2:1:10	254	225	29	11.4
50°C	282	257	25	8.9
80°C	285	239	46	16.1
Ethanol	316	288	28	8.9
Acetone	301	276	25	8.3
0.5:0.25:10	383	372	11	2.9
1:0.5:10	366	340	26	7.1

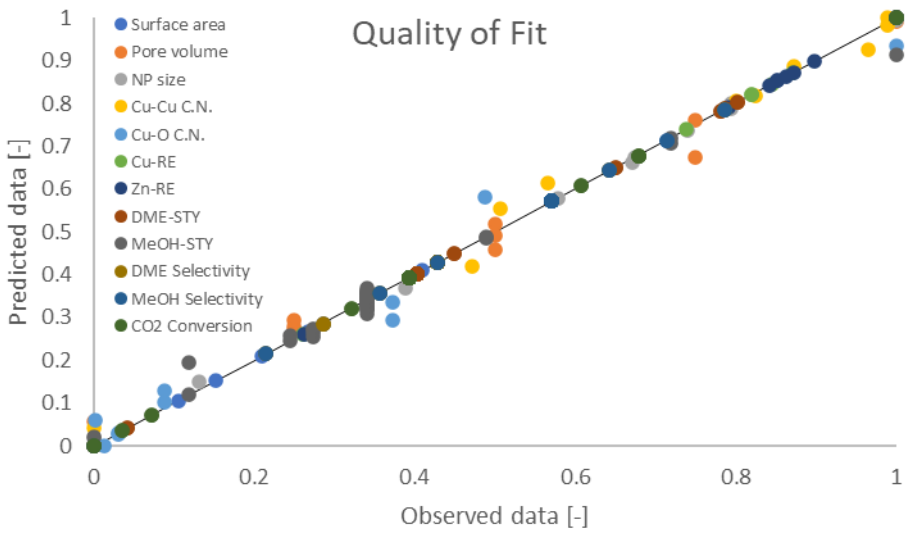

Fig. S12 Quality of fit which verifies that the model is able to reproduce experimentally observed results.

Table S7 Impact of preparation method of Cu^0-ZnO/SAPO-34 catalysts on the observed experimental catalyst performance.

Synthesis Method	DME MTY ($g_{DME}/kg_{Metal}/h$)	MeOH MTY ($g_{DME}/kg_{Metal}/h$)	DME Selectivity (%)	MeOH Selectivity (%)	Carbon Mass Balance (%)
15 mL	238	85	80	20	99
30 mL	370	136	79	21	100
45 mL /120°C/Water/2:1:10	443	174	78	22	97
50°C	100	39	77	23	101
80°C	114	55	74	26	100
Ethanol	323	76	85	15	98
Acetone	368	72	88	12	100
0.5:0.25:10	254	76	82	18	99
1:0.5:10	375	105	83	17	96

The average RSD between the triplicate repeat experiments for MTY is 17% and for selectivity it is 7%.

5 References

1 M. E. Potter, L. M. Armstrong and R. Raja, *Catal. Sci. Technol.*, 2018, **8**, 6163–6172.

2 B. Ravel and M. Newville, *J. Synchrotron Radiat.*, 2005, **12**, 537–541.